RSC Advances

PAPER

View Article Online
View Journal | View Issue

Cite this: *RSC Adv.*, 2021, **11**, 37498

Optical anticounterfeiting photonic bilayer film based on handedness of solid-state helicoidal structure†

Saddam Hussain,[a] Sajjad Haider,[b] Waheed Al-Masry[b] and Soo-Young Park *[a]

Received 19th September 2021
Accepted 12th November 2021

DOI: 10.1039/d1ra07021e

rsc.li/rsc-advances

Anticounterfeiting photonic bilayer films were fabricated by sandwiching two solid-state cholesteric liquid crystal films having different handedness. The fabricated photonic bilayer films were successfully applied to patterning by selective photopolymerization. This photonic bilayer film as a new cryptographic technology is of interest for its anticounterfeiting application.

Cryptography is a promising technology for information security, data encryption, anticounterfeiting, and camouflage. Widespread cryptographic technologies, such as holography,[1–4] watermarks,[5–8] and barcodes,[9–11] have been developed to authenticate commercial objects.[12,13] Shape memory polymers (SMPs) have been applied to encrypt information in the forms of letters, shapes, and other designs that can be disclosed after shape recovery.[14] Shape recovery and cryptography are used to create these encryptable SMPs. SMPs recover their shape in response to external stimuli such as heat and light. For example, a fluorescent shape memory hydrogel (SMH, one of the SMPs) has recently been reported. When heated, the SMH film flattened out and displayed encrypted fluorescent information under ultraviolet (UV) light.[15] These encryptable SMPs, however, could not be patched or stuck to the surfaces of commercial products to improve authentication availability and required some special instrumental setups to reveal the encrypted information. As a result, current cryptographic technologies with SMPs require more advanced technologies to improve commercial object authentication.

Nature is full of amazing chemical and physical colors. Unlike chemical colors obtained through the absorption of light by dyes and pigments, physical colors are generated by the interaction between light and periodically arranged microstructures with length scales comparable to the wavelengths of visible light. Photonic materials have emerged as an attractive material for the structural color's generation. Periodic structure of these materials allows them to reflect the ordinary light into specific color. There are so many approaches developed that can be used to generate structural color using one-, two- and three-dimensional photonic materials.[16–21] The physical colors are usually called structural colors, and those structures are called photonic crystals.[22–24] Compared to the colors from dyes and pigments, structural colors are durable and free from photobleaching. These attractive characteristics make structural colors of great value in practical applications and fuel a growing interest in fabricating artificial structural color materials.[25–28]

Cholesteric liquid crystals (CLCs) are one-dimensional photonic materials with self-organized periodic helical structures and a twist axis perpendicular to the local director.[29,30] The helicoidal photonic CLC structure can be fixed with a reactive CLC mixture after photopolymerization. The obtained solid-state CLC (CLC_{solid}) showed a perfect photonic structure with clear reflecting colors.[31] The photonic CLC reflects only right-handed (RH) or left-handed (LH) circularly polarized (CP) light depending on the used chiral dopant.[32] The RH (or LH) twisted helical structure can be generated by mixing an RH (or LH) chiral dopant with a nematic liquid crystal.[33,34] Thus, the CLC reflects only the circularly polarized light with the same handedness. The wavelength of the reflected light is governed by the Bragg relationship[35] of $\lambda = np\cos\theta$, where λ, n, p, and θ are wavelength at the photonic bandgap, average refractive index, helical pitch, and angle between the incident beam and the helical axis, respectively. Combining the RH and LH-CLC films with a multilayered structure can fabricate encrypted photonic films. In particular, the patterning at the selective part with different handedness enriches their anticounterfeiting applications.

Fig. 1a shows the chemical structures of commercially available materials used in this work. The procedures for preparing reactive RH-CLC and LH-CLC mixtures are as follows. The reactive RH-CLC mixture was prepared by mixing diacrylate mesogens RM82 (94 wt%), reactive RH chiral dopant LC756 (5 wt%), and photo-initiator Irgacure 500 (1 wt%) at 130 °C (>temperature at cholesteric to isotropic transition [T_{ChI}] = 110

[a]*School of Applied Chemical Engineering, Polymeric Nano Materials Laboratory, Kyungpook National University, Daegu, 41566, Republic of Korea. E-mail: psy@knu.ac.kr*

[b]*Chemical Engineering Department, College of Engineering, King Saud University, Riyadh 11421, Saudi Arabia*

† Electronic supplementary information (ESI) available. See DOI: 10.1039/d1ra07021e

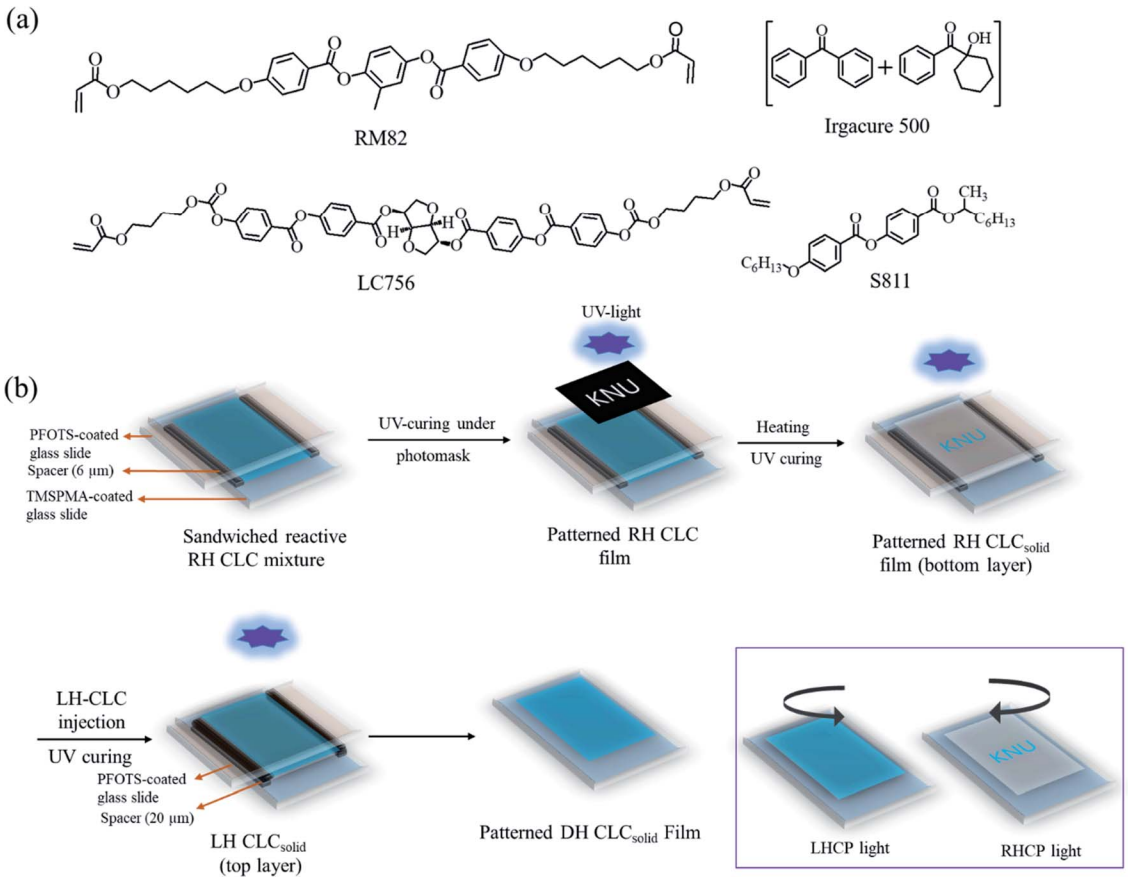

Fig. 1 (a) Chemical structures of diacrylate mesogens (RM82), reactive right-handed (RH) chiral dopant (LC756), nonreactive left-handed (LH) chiral dopant (S-811), and photo-initiator (Irgacure 500) used in the preparation of the reactive cholesteric liquid crystal (CLC) mixtures. (b) Schematic representation of the preparation procedure of the patterned dual-handed (DH) bilayer solid-state CLC (CLC_{solid}) film.

°C) under magnetic stirring (at 300 rpm) for 30 min and subsequently cooling down to 75 °C to obtain the CLC state. Similarly, the reactive LH-CLC mixture was prepared by mixing RM82 (74 wt%), nonreactive LH chiral dopant S-811 (25 wt%), and Irgacure 500 (1 wt%) under the same experimental conditions for preparing the reactive RH-CLC mixture except cooling down to 65 °C (instead of 75 °C) to obtain the CLC state because of its low T_{ChI} (101 °C). Fig. 1b displays the fabrication procedure of the bilayer CLC_{solid} film, with each layer having different handedness (dual-handed [DH] bilayer CLC_{solid} film). Briefly, the glass slides were cleaned thoroughly, washing with water and ethanol. After cleaning the glass slides, they were treated for 5 minutes with an oxygen plasma cleaner (CUTE, Femto Science, South Korea) to activate the surface of the glass slides for further functionalization. 3-(Trimethoxysilyl)propyl methacrylate (TMSPMA) was coated on the activated glass slide through a spin-coater (SPIN-1200D, Midas, South Korea) at 3000 rpm for 45 s and calcined at 100 °C for 10 min using an oven (DWO-G13SS, Daewoo, South Korea) to make TMSPMA-coated glass slides. Trichloro(1*H*,1*H*,2*H*,2*H*-perfluoroctyl) silane (PFOTS)-coated glass slides were prepared by keeping the activated glass slides in a sealed container containing an 8 μL PFOTS reagent *via* heating at 70 °C for 2 h using an oven (G1708A01090120, Daewoo, South Korea). A glass-slide cell with a 6 μm gap was prepared by fixing the PFOTS-coated glass slide on the TMSPMA-coated glass slide using micro pearl (6 μm in diameter) mixed in UV-curing glue (NOA65) followed by photopolymerization. The surface of the TMSPMA-coated glass slide contains reactive groups that could react with the reactive CLC mixtures, and the PFOTS-coated glass slide could be easily detached after polymerization. At 75 °C, the reactive RH-CLC mixture was capillary infiltrated to the 6 μm gap of the prepared glass-slide cell. After complete infiltration of the reactive RH-CLC mixture, selective UV curing (at 365 nm and 18 mW cm^{-2}, the same UV light was used for further experiments unless otherwise mentioned) was performed for 1 min under a photomask using a UV-curing machine (Innocure 100 N, Lichtzen, South Korea). Subsequently, the patterned RH-CLC film was heated up to 115 °C (>T_{ChI}), at which the unpolymerized part was turned to the isotropic state, and the patterned part remained in the RH-CLC_{solid} state. And then, the whole film was fully polymerized without a photomask under UV light for 10 min. The PFOTS-coated glass slide was detached from the patterned RH-CLC_{solid} film. By infiltrating the reactive LH-CLC mixture into the gap through capillary force at 65 °C, the second layer of the reactive LH-CLC mixture was fabricated with another PFOTS-coated glass slide on the bottom layer using a 20 μm double-sided adhesive plastic spacer. The top

layer of the reactive LH-CLC film was then UV-polymerized for 10 min before the PFOTS-coated glass slide was exposed. The unreacted chiral dopant of CB15 was washed out with acetone several times. The obtained bilayer DH-CLC_{solid} film is 20 and 6 μm thick at the bottom and top layers.

The single-layer CLC_{solid} films with the same RH and LH reactive CLC mixtures were fabricated to study the effect of the handedness on the cryptographic property of the DH-CLC_{solid} film. Fig. 2a displays the microscopic images of the single-layer RH and LH CLC_{solid} films under ordinary, right-handed circularly polarized (RHCP), and left-handed circularly polarized (LHCP) lights. The single-layer RH and LH CLC_{solid} films reflect blue colors under ordinary light and the same-handed light. However, the single-layer RH and LH CLC_{solid} films do not reflect under oppositely handed lights. Fig. 2b exhibits the UV-vis spectra of the single-layer RH and LH CLC_{solid} films, respectively, under ordinary, RHCP, and LHCP lights. A UV-vis spectrophotometer (DH-2000-BAL, Ocean Optics, USA) recorded the UV-vis spectra in the 300–900 nm range. RHCP and LHCP lights were achieved by putting a quarter-wave plate and a polarizer in the front of an incident light beam. As a result, the single-layer RH and LH CLC_{solid} films show the strong photonic band gap (PBG) under corresponding RHCP and LHCP lights with their well-established PBG edges but little reflection under oppositely handed lights. Thus, these single-layer RH and LH CLC_{solid} films could be applied to develop the optical anti-counterfeiting photonic film by combining these two single-handed CLC_{solid} layers with different handedness. The wavelengths at photonic band gaps (λ_{PBG}s) of the RH and LH CLC_{solid} films are 475 and 470 nm, respectively, consistent with the colors observed from the photographic images in Fig. 2a. The chiral dopant used in the fabrication of the RH and LH CLC_{solid} films are LC756 and S811, which are reactive and non-reactive ones, respectively. The reactive chiral dopant of LC756 has the same kind of reactive acryl groups so that the dimensional stability of the RH CLC_{solid} film may be better than that of the LH CLC_{solid} film with the non-reactive chiral dopant of S811. The width of band edge is also strongly dependent on the

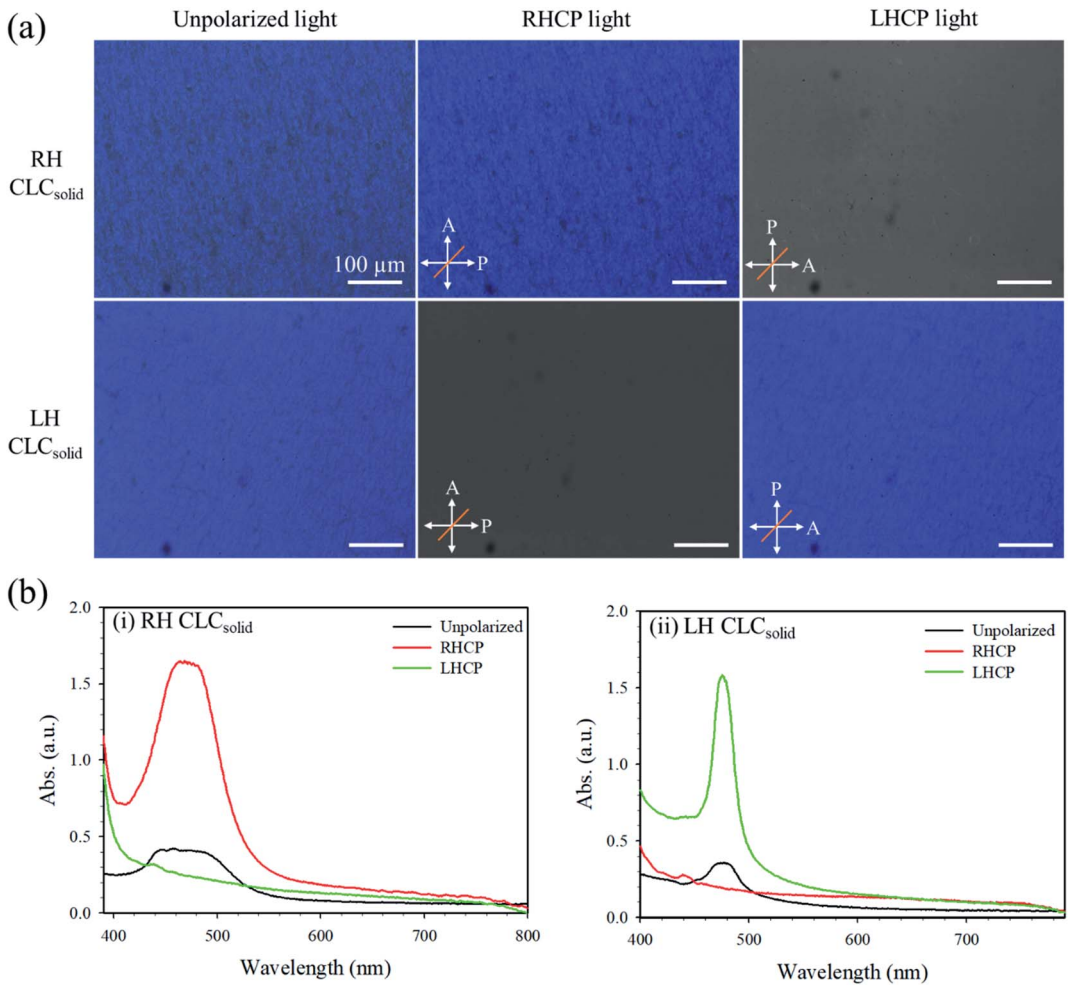

Fig. 2 (a) Microscopic images (in reflection mode) and (b) UV-vis spectra of the single-layer (i) right-handed (RH) and (ii) left-handed (LH) solid-state cholesteric liquid crystal (CLCsolid) films under ordinary, right-handed circularly polarized (RHCP), and left-handed circularly polarized (LHCP) lights. The given scale bar in (a) is 100 μm for all images. A and P arrows in (a) indicate the directions of analyzer and polarizer, respectively, and orange line is for the direction of a quarter-wave plate.

difference between ordinary and extraordinary reflective indices of the used chiral dopant. The defect in the photonic structure can broaden the width of the photonic bandgap so that the rectangular shape of the photonic bandgap is lost in the case of the LH CLC_{solid} film when the non-reactive chiral dopant is used. It is well known that there is a forbidden stopband for light propagating along the axis of the helix with pitch P in the spectral range $n_{\|}P \geq \lambda \geq n_{\perp}P$ ($n_{\|}$ and $n_{\perp}$ are the principal refractive indices parallel and perpendicular to the liquid crystal director, respectively). In the spectral range of the stopband, the propagation of circularly polarized light of the same handedness as that of the helix is forbidden[36,37] and it experiences Bragg reflection from the CLC layer.

The cross-sectional surfaces of patterned and isotropic parts of the bottom RH-CLC_{solid} film were analyzed using field emission scanning electron microscopy (FE-SEM, SU8220, Hitachi, Japan). Fig. S1a(i)† shows the SEM image of the cross-sectional surface of the patterned part of the RH-CLC_{solid} film. The pitch (p) of the RH-CLC_{solid} film was measured 3 times at random positions. The obtained average pitch was 305 nm. The λ_{PBG} was calculated from the pitch using the following equation of $\lambda_{PBG} = np$, where p is the helical pitch (305 nm) and n is refractive index (1.54).[38] The calculated λ_{PBG} was 469 nm which is close to the λ_{PBG} (475 nm) determined from the UV-vis spectrum (Fig. 2b(i)). Fig. S1a(ii)† exhibits the SEM image of the cross-sectional surface of the isotropic part. It shows the plain structure without helical or layered one, indicating that the isotropic structure was obtained in the background of the RH-CLC_{solid} film. The structures of the RH, LH and DH-CLC_{solid} films were also studied using Fourier transform infrared (FTIR) spectroscopy (FT/IR-4100, Jasco, Japan) as shown in Fig. S1b.† The peaks at 1728, 1609 and 1510 cm^{-1} were commonly observed from all three samples, attributing to the carbonyl (C=O) stretching band, carbon–carbon (C–C) stretching, and another carbon–carbon (C–C) stretching band of the aromatic rings of the RM82 mesogen, respectively.[39,40] The characteristic peaks at 1204 and 667 cm^{-1} in the spectrum of the LH-CLC_{solid} film (Fig. S1b(ii)†) attribute to the O–C stretching and C–H bending of the chiral dopant S-811, respectively.[41,42] The same characteristic peaks were observed in the spectrum of the DH CLC_{solid} film, indicating that the bilayer DH CLC_{solid} film was successfully formed with LH and RH chiral dopants.

Patterned photonic bilayer DH-CLC_{solid} films were fabricated by sandwiching the two CLC_{solid} films having different handedness but similar λ_{PBG} (475 and 470 nm at the bottom and top layers, respectively) after selective UV curing of the bottom layer under different photomasks. Fig. 3a shows the schematic representation of the internal structure and handedness of the fabricated DH-CLC_{solid} film. The patterned bottom layer was made of the RH-CLC_{solid} film at the selective area with isotropic background, and the plain top layer was made of the LH CLC_{solid} film without patterning. Thus, the patterned part consists of the RH (bottom layer) and LH (top layer) CLC_{solid} structure, and the background is made of the isotropic (bottom layer) and LH (top layer) CLC_{solid} structure. Fig. 3b(i) exhibits the photographic images of the dot pattern under unpolarized, RHCP, and LHCP lights. The dot pattern is only visible in RHCP

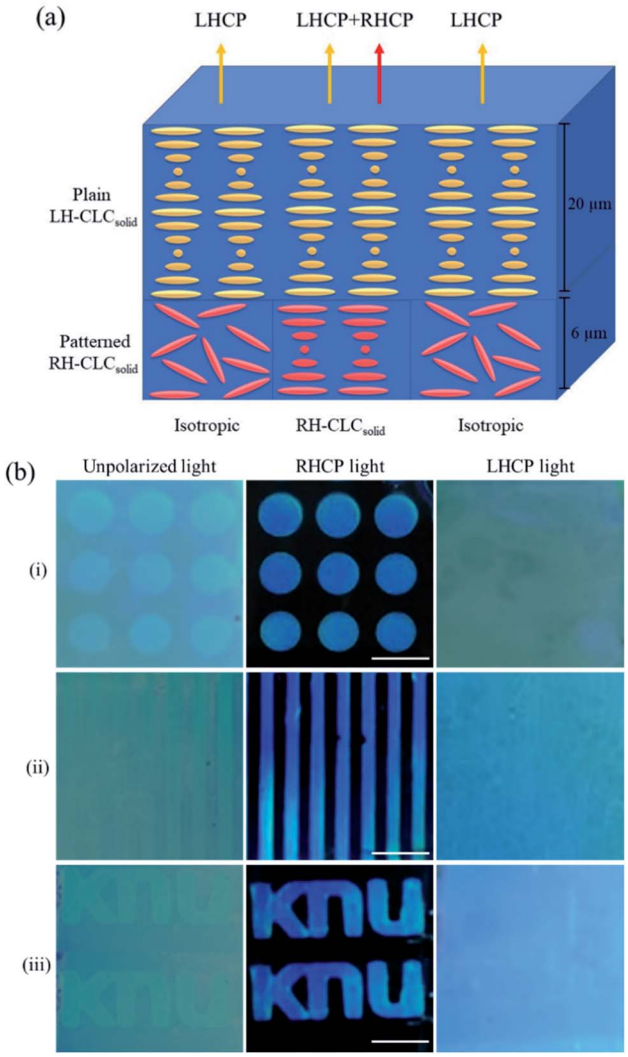

Fig. 3 (a) Schematic representation of the internal structure and handedness of the fabricated double-handed (DH)-solid-state cholesteric liquid crystal (CLC_{solid}) film. (b) Photographic images of the (i) dots, (ii) lines, and (iii) "KNU" letter patterns of the DH-CLC_{solid} films under unpolarized, right-handed circularly polarized (RHCP), and left-handed circularly polarized (LHCP) lights. The scale bars are 4 mm.

light because the patterned part of the bottom layer reflects only RHCP light, whereas it is invisible in LHCP light because only the top plain LH CLC_{solid} layer is reflected. However, the patterned part is slightly visible against the background in an unpolarized beam due to the thickness difference of the CLC_{solid} layer between the patterned and background parts. Similarly, the other patterns with line and "KNU" letters were demonstrated in Fig. 3b(ii) and (iii). The long-term stability of the DH-CLC_{solid} film was tested with the dotted pattern of the DH-CLC_{solid} film. Fig. S2a† shows the photographic images (under unpolarized, RHCP and LHCP lights) of the freshly prepared dot pattern of the DH-CLC_{solid} film which were compared with the same film 56 days after preparation (Fig. S2b†). The dot pattern of the DH-CLC_{solid} film is clearly visible even 56 days after the preparation, indicating that the

corresponding film have long term stability without any significant loss in its photonic property. This photonic bilayer film can be applied to fabricate circular-polarizing reflective mirrors on the simple polarizer glasses. One of the disadvantages in using the CLC structure for anticounterfeiting application is the dependency of the reflected color on the viewing angle; the reflected color of the flat film of the CLC structure is strongly dependent on the viewing angle so that the observed patterned color can be changed depending on the observation direction. The DH-CLC_{solid} film is also non-stretchable so that it is difficult to patch it on the commercial object by simple stretching like vinyl wraps.

The photonic CLC structure can induce unique handedness properties depending on the used chiral dopant. This cryptographic technology based on the DH bilayer structure can be easily applied with commercially applied materials and simple photopolymerization with designed photo masks on a rigid or flexible substrate. The commercially available raw materials can be beneficial to the commercialization of the CLC_{solid} film for anticounterfeit, data encryption, and authentication of commercial objects with low cost.

Conclusions

This study demonstrates the bilayer DH-CLC_{solid} film's handedness-dependent photonic property. When the pattern is encrypted in one layer, the bilayer CLC_{solid} film with two different RH and LH handednesses generates an anticounterfeiting pattern. The pattern is only visible when the patterned layer's corresponding CP light is turned on. The bilayer CLC_{solid} film's potential commercialization is aided by its simple fabrication method, commercially available raw materials, versatility, and readability with simple polarizer glasses.

Author contributions

Saddam Hussain, Sajjad Haider, Waheed Al-Masry and Soo-Young Park designed the study and interpreted all the results. Saddam Hussain fabricated the optical photonic bilayer films and conducted the experiments. Soo-Young Park supervised the current work. All authors analyzed the data. Saddam Hussain and Soo-Young Park wrote the manuscript.

Conflicts of interest

The authors declare no competing financial interest.

Acknowledgements

This work was supported by the National Research Foundation of Korea (2020R1A2B5B02001556). The authors extend their appreciation to the Deputyship for Research & Innovation, Ministry of Education in Saudi Arabia for funding this research work through the project number (DRI-KSU-637).

References

1 H. Nam, K. Song, D. Ha and T. Kim, *Sci. Rep.*, 2016, **6**, 1–9.
2 J. Chambers, W. Yan, A. Garhwal and M. Kankanhalli, *Multimed. Tools. Appl.*, 2015, **74**, 4013–4043.
3 I. H. Lee, G. Li, B. Y. Lee, S. U. Kim, B. Lee, S. H. Oh and S. D. Lee, *Opt. Express*, 2019, **27**, 24512–24523.
4 K. Huang, J. Deng, H. S. Leong, S. L. K. Yap, R. B. Yang, J. Teng and H. Liu, *Laser Photonics Rev.*, 2019, **13**, 1800289.
5 S. Huang and J. K. Wu, *IEEE Trans. Inf. Forensics Secur.*, 2007, **2**, 164–173.
6 W. Yao, R. Lan, K. Li and L. Zhang, *ACS Appl. Mater. Interfaces*, 2021, **13**, 1424–1430.
7 H. Hu, H. Zhong, C. Chen and Q. Chen, *J. Mater. Chem. C*, 2014, **2**, 3695–3702.
8 M. Wang, Y. Xu, H. Tan, L. Xu, C. Zhang and J. Xu, *Nanosci. Nanotechnol. Lett.*, 2018, **10**, 365–372.
9 S. Han, H. J. Bae, J. Kim, S. Shin, S. E. Choi, S. H. Lee, S. Kwon and W. Park, *Adv. Mater.*, 2012, **24**, 5924–5929.
10 R. Xie, C. Hong, S. Zhu and D. Tao, *Neurocomputing*, 2015, **167**, 625–635.
11 W. S. Li, Y. Shen, Z. J. Chen, Q. Cui, S. S. Li and L. j. Chen, *Appl. Opt.*, 2017, **56**, 601–606.
12 R. Arppe and T. J. Sørensen, *Nat. Rev. Chem.*, 2017, **1**, 1–13.
13 Y. Lin, H. Zhang, J. Feng, B. Shi, M. Zhang, Y. Han, W. Wen, T. Zhang, Y. Qi and J. Wu, *Small*, 2021, e2100244.
14 L. Sun, T. X. Wang, H. M. Chen, A. V. Salvekar, B. S. Naveen, Q. Xu, Y. Weng, X. Guo, Y. Chen and W. M. Huang, *Polymers*, 2019, **11**, 1049.
15 C. N. Zhu, T. Bai, H. Wang, J. Ling, F. Huang, W. Hong, Q. Zheng and Z. L. Wu, *Adv. Mater.*, 2021, 2102023.
16 Y. Yue and J. P. Gong, *Photochem. Rev.*, 2015, **23**, 45–67.
17 J. Pei, J. Yang, T. Yildirim, H. Zhang and Y. Lu, *Adv. Mater.*, 2019, **31**, 1706945.
18 J. He, L. Tao, H. Zhang, B. Zhou and J. Li, *Nanoscale*, 2019, **11**, 2577–2593.
19 X. Qi, Y. Zhang, Q. Ou, S. T. Ha, C. W. Qiu, H. Zhang, Y. B. Cheng, Q. Xiong and Q. Bao, *Small*, 2018, **14**, 1800682.
20 T. Tan, X. Jiang, C. Wang, B. Yao and H. Zhang, *Adv. Sci.*, 2020, **7**, 2000058.
21 R. K. Cersonsky, J. Antonaglia, B. D. Dice and S. C. Glotzer, *Nat. Commun.*, 2021, **12**, 1–7.
22 V. Sharma, M. Crne, J. O. Park and M. Srinivasarao, *Science*, 2009, **325**, 449–451.
23 F. Fu, L. Shang, Z. Chen, Y. Yu and Y. Zhao, *Sci. Robot.*, 2018, **3**, DOI: 10.1126/scirobotics.aar8580.
24 P. Vukusic and J. R. Sambles, *Nature*, 2003, **424**, 852–855.
25 C. Lopez, *Adv. Mater.*, 2003, **15**, 1679–1704.
26 A. J. Kragt, D. C. Hoekstra, S. Stallinga, D. J. Broer and A. P. Schenning, *Adv. Mater.*, 2019, **31**, 1903120.
27 M. G. Han, C. G. Shin, S. J. Jeon, H. Shim, C. J. Heo, H. Jin, J. W. Kim and S. Y. Lee, *Adv. Mater.*, 2012, **24**, 6438–6444.
28 J. Ge and Y. Yin, *Angew. Chem., Int. Ed.*, 2011, **50**, 1492–1522.
29 M. Mitov, *Adv. Mater.*, 2012, **24**, 6260–6276.
30 S. Hussain and S. Y. Park, *ACS Sens.*, 2020, **5**, 3988–3998.

31 D. B. Myung, S. Hussain and S. Y. Park, *Sens. Actuators, B*, 2019, **298**, 126894.
32 N. Tamaoki, *Adv. Mater.*, 2001, **13**, 1135–1147.
33 S. Hussain and S. Y. Park, *Sens. Actuators, B*, 2020, **316**, 128099.
34 V. Belyakov, V. E. Dmitrienko and V. P. Orlov, *Sov. Phys. Usp.*, 1979, **22**, 64.
35 W. S. John, W. Fritz, Z. Lu and D. K. Yang, *Phys. Rev. E: Stat. Phys., Plasmas, Fluids, Relat. Interdiscip. Top.*, 1995, **51**, 1191.
36 L. M. Blinov, *Structure and properties of liquid crystals*, Springer Science & Business Media, 2010.
37 V. A. Belyakov, *Diffraction optics of complex-structured periodic media*, Springer, 1992.
38 H. Ren, S. Xu and S. T. Wu, *Opt. Express*, 2012, **20**, 26464–26472.
39 K. Noh and S. Y. Park, *Mater. Horiz.*, 2017, **4**, 633–640.
40 H. Einaga, K. Mochiduki and Y. Teraoka, *Catalysts*, 2013, **3**, 219–231.
41 Y. Liu and H. J. Kim, *Sens.*, 2017, **17**, 1469.
42 N. Atykyan, V. Revin and V. Shutova, *AMB Express*, 2020, **10**, 1–11.